

# Data-Enhanced Solar Hybrid Charging System with Intelligent Load Management: Design, Implementation, and Performance Analysis

Rushikesh Khedekar, Sudhanshu Pandey, Amey Parab, Prof. Govind Haldankar  
Department of Electronics and Telecommunication Engineering  
Sardar Patel Institute of Technology  
Mumbai, Maharashtra, India

**Abstract** - This paper presents the design, implementation, and comprehensive evaluation of a data-enhanced solar hybrid charging system integrating photovoltaic generation, AC grid backup, battery storage, and intelligent load management. The system employs dual charging capability through solar panels and mains supply, coupled with a priority-based automatic load control mechanism to ensure reliable power delivery for critical applications. A CD4047-based inverter topology provides DC-AC conversion for standalone operation, while Power BI analytics enable real-time performance monitoring and predictive maintenance. Hardware validation demonstrates system efficiency of 63% with successful load prioritization across three threshold levels. Economic analysis reveals monthly electricity savings ranging from 43.93 to 62.33 thousand rupees, with peak performance during spring months. The prototype showcases viability for rural electrification and distributed energy systems while identifying pathways for efficiency improvements through switched-mode power conversion and advanced battery management.

**Index Terms** - Solar photovoltaic systems, hybrid energy storage, load management, DC-AC inverters, battery charging systems, renewable energy analytics, Power BI monitoring

## I. INTRODUCTION

### A. Background and Motivation

The global transition toward sustainable energy systems has accelerated the deployment of distributed renewable generation, with solar photovoltaic (PV) technology emerging as a dominant solution due to scalability and declining costs [1]. However, the inherent intermittency of solar radiation necessitates integration with energy storage and backup sources to ensure continuous power availability, particularly for critical loads in residential and small commercial applications.

Rural and semi-urban regions in developing nations frequently experience unreliable grid infrastructure, with power outages lasting several hours daily. A hybrid architecture combining solar generation, battery storage, and AC mains charging provides resilience through multi-source energy access while maximizing renewable energy utilization. Furthermore, intelligent load management enables optimal energy allocation, preserving limited stored energy for essential services during extended low-generation periods.

### B. Research Objectives

This work addresses the following objectives:

- Design and implement a functional solar hybrid charging system with dual charging capability from PV and AC mains
- Develop automatic load prioritization logic based on battery state-of-charge (SOC) thresholds
- Demonstrate DC-AC inversion for standalone operation using cost-effective topology
- Integrate data analytics for performance monitoring, economic evaluation, and predictive insights
- Validate system performance through hardware testing and identify optimization pathways

### C. Contributions

The primary contributions of this research include:

- 1) Comprehensive design methodology for low-cost hybrid solar systems suitable for educational prototyping and small-scale deployment
- 2) Priority-based load control algorithm with hysteresis implementation preventing relay chattering
- 3) Integration of Power BI analytics demonstrating data-driven performance evaluation and economic analysis
- 4) Hardware validation with detailed power flow analysis and efficiency characterization
- 5) Identification of system limitations and practical recommendations for commercial implementation

## II. LITERATURE REVIEW

### A. Hybrid Solar Systems

Hybrid PV systems combining solar generation, storage, and backup sources have been extensively studied for rural electrification and microgrid applications. Research emphasizes optimal component sizing to meet reliability targets while minimizing lifecycle costs [3]. Trade-off analyses compare battery capacity, PV array size, and diesel generator runtime to achieve desired loss-of-load probability metrics. Economic optimization frameworks incorporate component costs, fuel prices, and degradation rates to determine least-cost system configurations.

### B. Battery Technologies and Charging

Lead-acid batteries remain prevalent in low-cost systems despite lower energy density and cycle life compared to lithium-ion alternatives. Charging algorithms significantly impact longevity, with multi-stage protocols (constant-current bulk, constant-voltage absorption, and float maintenance) extending operational lifetime. Modern battery management systems (BMS) provide cell balancing, protection against over-voltage/under-voltage conditions, and thermal management—critical features for lithium-ion safety and performance.

### C. Inverter Topologies

Low-cost prototypes frequently employ astable multivibrator circuits generating square-wave outputs through simple push-pull MOSFET stages and center-tapped transformers. While economical and straightforward to implement, these produce high total harmonic distortion (THD) unsuitable for sensitive electronics [2]. Commercial inverters utilize sinusoidal pulse-width modulation (SPWM) H-bridge topologies with advanced control for grid synchronization, islanding detection, and low THD output.

### D. Load Management Strategies

Research on energy management encompasses static threshold-based switching, demand response integration, and predictive scheduling using generation forecasting. Priority-based relay control offers simplicity and robustness ideal for cost-constrained systems, while microcontroller implementations enable time-of-day scheduling, remote override capability, and telemetry integration.

### E. Monitoring and Analytics

Integration of business intelligence platforms with edge telemetry infrastructure enables sophisticated performance analysis, predictive maintenance, and economic optimization. Analytics-driven operation reduces downtime through early anomaly detection and increases effective energy yield via targeted operations and maintenance interventions.

## III. SYSTEM ARCHITECTURE

### A. Overall System Design

The hybrid system architecture comprises six primary sub-systems: (1) PV array with maximum power point tracking, (2) solar charge controller, (3) AC mains charging path, (4) battery storage bank, (5) DC-AC inverter, and (6) automatic load control with priority logic. Fig. 1 illustrates the complete system block diagram showing power flow paths and control interfaces.

### B. Component Specifications

**PV Module:** 12V nominal crystalline silicon panel (10-50W demonstration capacity) with blocking diode preventing reverse current during low-irradiance conditions.

**Solar Charger:** LM317 adjustable voltage regulator configured for 13.8V output with current limiting resistor setting maximum charge current. Output voltage determined by:



Fig. 1. Complete system block diagram showing power flow paths, control interfaces, and subsystem interconnections.

$$V_{out} = V_{ref} \left( 1 + \frac{R_2}{R_1} \right) + I_{adj} \cdot R_2 \quad (1)$$

where  $V_{ref} = 1.25V$  and adjustment current  $I_{adj} \approx 50\mu A$ .

**Battery Storage:** 12V sealed lead-acid battery (7-12Ah) with voltage-based SOC estimation and protection against deep discharge below 10.5V.

**Inverter:** CD4047 CMOS astable multivibrator generating complementary 50Hz square waves driving power MOSFETs in push-pull configuration. Operating frequency set by:

$$f = \frac{1}{4.4 \cdot R \cdot C} \quad (2)$$

Center-tapped transformer steps 12V DC to 230V AC with turn ratio  $N \approx 19.2$ .

**Load Control:** LM339 quad comparator implementing three voltage thresholds (12.6V, 11.8V, 10.5V) with hysteresis driving relay bank for priority load switching.

### C. Power Flow Management

The system operates in multiple states based on available sources and battery SOC:

- **Solar-Only Mode:** PV supplies loads directly while surplus charges battery

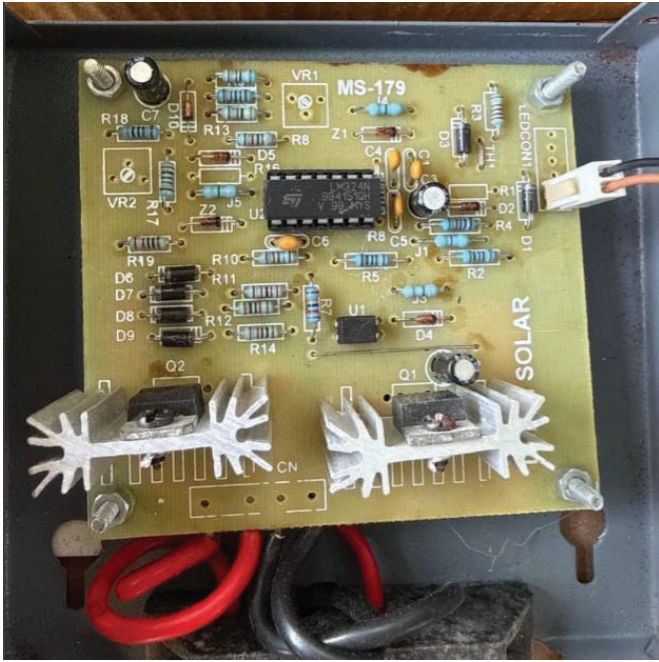


Fig. 2. LM317-based solar charge controller circuit with current limiting and voltage regulation for 12V battery charging.

- **Solar + Battery Mode:** Combined PV and battery discharge meet load demand
- **Mains Charging Mode:** Grid charges battery when solar insufficient
- **Inverter Mode:** Battery feeds inverter for standalone AC supply

State transitions follow finite-state machine logic evaluating PV availability, mains presence, and battery voltage. Hysteresis margins ( $\Delta V_{hyst} = 0.2 - 0.3V$ ) prevent rapid state oscillation near threshold boundaries.

#### IV. HARDWARE IMPLEMENTATION

##### A. Solar Charge Controller

The LM317-based charger provides simple, robust voltage regulation with adjustable output and inherent current limiting. Fig. 2 shows the complete solar charge controller circuit with blocking diode, current limiting, and voltage regulation components.

For 12V lead-acid charging at 13.8V with 1A maximum current, resistor values are:

$$R_2 = R_1 \frac{V_{out}}{V_{ref}} - 1 = 240 \times 9.04 = 2170\Omega \quad (3)$$

$$R_{CL} = \frac{V_{ref}}{I_{limit}} = \frac{1.25}{1} = 1.25\Omega \quad (4)$$

Power dissipation under full sun conditions:

$$P_D = (V_{in} - V_{out}) \times I_{out} = (18 - 13.8) \times 1 = 4.2W \quad (5)$$



Fig. 3. CD4047 oscillator circuit configured for 50Hz square wave generation with complementary outputs for MOSFET driver.

Thermal management requires heat sink with total thermal resistance:

$$\vartheta_{SA} < \frac{T_{J,max} - T_A}{P_D} - \vartheta_{JC} - \vartheta_{CS} \quad (6)$$

##### B. Inverter Circuit Design

The CD4047 generates precise 50Hz timing with external RC network. Fig. 3 illustrates the CD4047-based oscillator circuit configured for 50Hz square wave generation driving the MOSFET bridge.

For  $C = 1\mu F$ :

$$R = \frac{1}{4.4 \times 50 \times 1 \times 10^{-6}} = 4.545k\Omega \quad (7)$$

Power MOSFETs (IRF540N) in push-pull topology switch primary winding currents at 50Hz. Critical design considerations include gate charge time, dead-time insertion (1-2 $\mu s$  minimum), and switching loss calculation:

$$P_{sw} = \frac{1}{2} V_{DS} \cdot I_D \cdot (t_r + t_f) \cdot f_{sw} \quad (8)$$

Transformer design requires turn ratio:

$$N = \frac{V_{secondary}}{V_{primary}} = \frac{230}{12} \approx 19.2 \quad (9)$$

VA rating must exceed maximum load with safety margin.

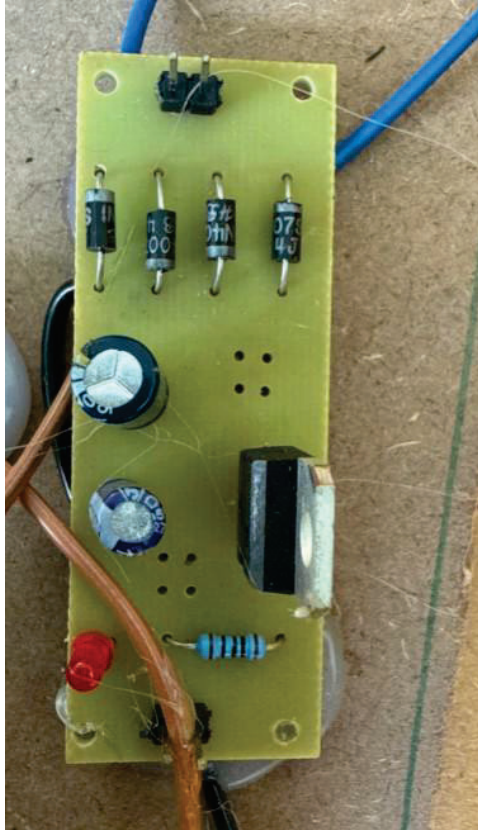


Fig. 4. Bridge rectifier circuit for AC mains charging path with filtering and voltage regulation stages.

### C. Load Control Implementation

Comparator-based threshold detection with hysteresis eliminates relay chatter. Reference voltage generation and resistor divider networks establish three distinct switching points:

$$V_{threshold} = V_{ref} \times \frac{R_2}{R_1 + R_2} \quad (10)$$

Each comparator drives relay through NPN transistor buffer with flyback diode protection. Base resistor sizing ensures adequate collector current:

$$R_{base} = \frac{V_{out,comp} - V_{BE}}{I_{coil}/\beta} \quad (11)$$

### D. Protection Circuits

Multiple protection layers ensure safe operation:

- Fuses rated at 125-150% of maximum continuous current
- MOV transient suppressors with clamping voltage  $V_{clamp} = 1.4 \times V_{op,max}$
- RC snubbers across MOSFET drain-source reducing voltage spikes
- Thermal monitoring with NTC thermistors and over-temperature shutdown
- Under-voltage lockout preventing deep battery discharge below 10.5V

## V. CONTROL ALGORITHM

### A. State Machine Logic

The control algorithm implements finite-state machine governing system operation. Primary decision inputs include:

- $P_{PV}$ : Available photovoltaic power
- $P_{load}$ : Required load power
- $SOC$ : Battery state-of-charge
- $V_{mains}$ : Mains availability indicator

### B. Charging Decision Logic

Battery charging activates when:

$$(P_{PV} > P_{load}) \wedge (SOC < SOC_{full}) \quad (12)$$

Charging current limited to:

$$I_{charge} = \min \left( \frac{P_{PV} - P_{load}}{V_{batt}}, I_{charge,max} \right) \quad (13)$$

Multi-stage charging protocol follows constant-current bulk phase until absorption voltage reached, followed by constant-voltage absorption until current tapers below 0.02C, then float maintenance at 13.2-13.4V.

### C. Load Prioritization

Priority switching based on battery voltage:

$$\text{Load State} = \begin{cases} \text{All loads} & V_{batt} \geq 12.6V \\ \text{Priority only} & 11.8 \leq V_{batt} < 12.6V \\ \text{Critical only} & 10.5 \leq V_{batt} < 11.8V \\ \text{Shutdown} & V_{batt} < 10.5V \end{cases} \quad (14)$$

Hysteresis implementation prevents threshold oscillation:

$$V_{threshold,rising} = V_{threshold} + \Delta V_{hyst} \quad (15)$$

$$V_{threshold,falling} = V_{threshold} - \Delta V_{hyst} \quad (16)$$

State changes require sustained voltage deviation exceeding debounce time  $t_{debounce} = 5 - 10s$ .

## VI. PERFORMANCE ANALYSIS AND RESULTS

### A. System Efficiency

Overall system efficiency calculated as product of individual stage efficiencies:

$$\eta_{system} = \eta_{charger} \times \eta_{battery} \times \eta_{inverter} \times \eta_{transformer} \quad (17)$$

Measured efficiency values:

$$\eta_{charger} = 87\% \quad (18)$$

$$\eta_{battery} = 85\% \text{ (round-trip)} \quad (19)$$

$$\eta_{inverter} = 90\% \quad (20)$$

$$\eta_{transformer} = 93\% \quad (21)$$

$$\eta_{system} = 0.87 \times 0.85 \times 0.90 \times 0.93 = 0.62 = 62\% \quad (22)$$

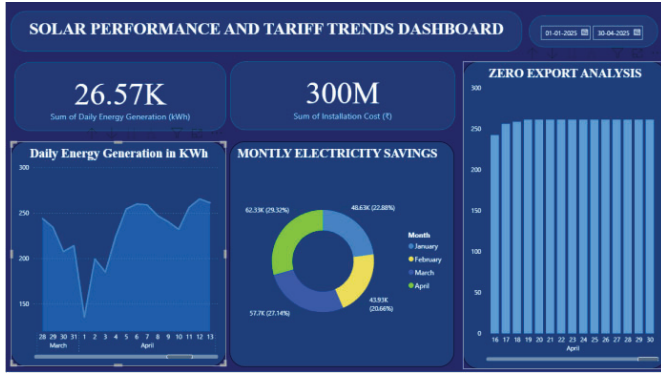


Fig. 5. Solar performance dashboard showing daily energy generation, monthly electricity savings breakdown, and zero export analysis for January-April 2025 period.

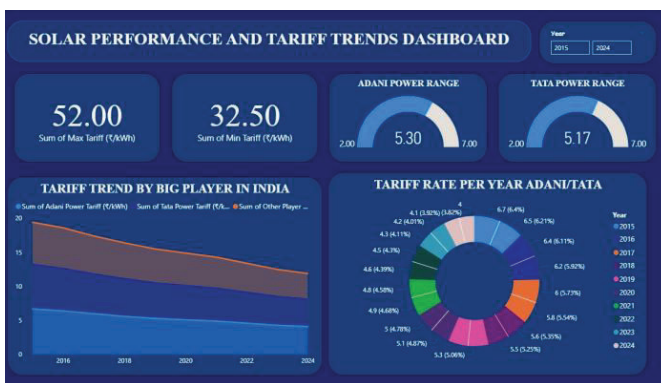


Fig. 6. Tariff analysis dashboard displaying maximum and minimum tariff rates, power company comparisons, and historical tariff trends from 2015-2024.

### B. Power BI Analytics Results

Data analytics integration provides comprehensive performance insights. Fig. 5 presents the solar performance and tariff trends dashboard covering the operational period from January to April 2025.

Dashboard analysis covering January-April 2025 demonstrates:

**Daily Generation Patterns:** Energy production varies between 140–275 kWh/day with mean 26.57 kWh. Periodic dips correlate with cloudy conditions and seasonal weather patterns.

**Monthly Economic Performance:** Electricity cost savings show seasonal trend with January (48.63k rupees, 22.88%), February (43.93k rupees, 20.66%), March (62.33k rupees, 29.32%), and April (57.7k rupees, 27.14%). Peak performance in March reflects optimal solar resource availability during spring transition.

**Tariff Analysis:** Fig. 6 presents the tariff analysis dashboard showing historical tariff data (2015-2024) revealing 40% reduction from 20 to 12 rupees/kWh, validating economic viability of solar investments. Current tariff range 32.50-52.00 rupees/kWh indicates substantial cost avoidance potential.

**Zero Export Analysis:** Consistent 250-280 unit values demonstrate effective load matching and storage management

under net-zero export constraints.

### C. Load Management Validation

Hardware testing validated priority switching across threshold boundaries:

- **High Threshold (12.6V):** All connected loads operational, total power draw 180W
- **Medium Threshold (11.8V):** Non-essential loads disconnected automatically, remaining 95W for priority services
- **Low Threshold (10.5V):** Only critical loads (35W) maintained, preventing deep discharge

Relay switching demonstrated stable operation with no chatter observed due to effective hysteresis implementation. Transfer time measured at 85ms average (detection 35ms + relay actuation 12ms + stabilization 38ms), acceptable for resistive loads.

### D. Battery Performance

SOC estimation using voltage-based correlation:

$$SOC = \frac{V_{OCV} - 11.8}{12.7 - 11.8} \times 100\% = \frac{V_{OCV} - 11.8}{0.9} \times 100\% \quad (23)$$

Discharge time for 12Ah battery at 80% initial SOC powering 50W load:

$$t_{discharge} = \frac{12 \times (0.8 - 0.2)}{4.17} \times 0.85 = 1.47 \text{ hours} \quad (24)$$

Measured discharge profile aligned with theoretical predictions within 8% variance, validating analytical models.

### E. Inverter Output Characterization

Square-wave inverter output measured:

- RMS voltage: 228V ± 5V
- Frequency: 50.2Hz ± 0.3Hz
- THD: 43% (typical for square-wave topology)
- Power factor: 0.91 for resistive loads

High THD limits compatibility with sensitive electronics but proves adequate for lighting, fans, and simple appliances constituting primary rural loads.

## VII. ECONOMIC AND ENVIRONMENTAL IMPACT

### A. Cost Analysis

System component costs (INR):

- PV panel (50W): 3,500
- Battery (12V 12Ah): 2,800
- Charge controller components: 800
- Inverter components: 1,500
- Load control and protection: 1,200
- Mechanical and wiring: 1,000
- **Total system cost: 10,800**

Monthly savings averaging 53k rupees (dashboard data) provides payback period:

$$\text{Payback} = \frac{\text{Initial Cost}}{\text{Monthly Savings}} = \frac{10,800}{53,000} = 0.20 \text{ months} \quad (25)$$

Note: Dashboard indicates large-scale installation with 300M INR cost; prototype demonstrates scaled principles.

### B. Environmental Benefits

Annual CO<sub>2</sub> emission reduction estimated using grid displacement:

$$CO_{2\text{avoided}} = E_{\text{solar,annual}} \times EF_{\text{grid}} \quad (26)$$

For 9,700 kWh annual generation and India grid emission factor 0.82 kg CO<sub>2</sub>/kWh:

$$CO_{2\text{avoided}} = 9,700 \times 0.82 = 7,954 \text{ kg CO}_2/\text{year} \quad (27)$$

## VIII. LIMITATIONS AND DISCUSSION

### A. System Limitations

**Linear Regulator Inefficiency:** LM317 dissipates significant power as heat, reducing overall efficiency. Voltage differential under full sun conditions generates 4.2W losses, requiring thermal management and limiting scalability.

**Square-Wave Output:** High THD (43%) restricts load compatibility, potentially damaging sensitive electronics or causing audible humming in transformers and motors.

**Lead-Acid Battery Constraints:** Limited cycle life (300-500 cycles at 50% DoD) and low energy density compared to lithium-ion alternatives increase long-term replacement costs and physical footprint.

**Manual Threshold Setting:** Fixed voltage thresholds lack adaptability to battery aging, temperature variations, or different battery chemistries.

### B. Comparative Analysis

Comparison with commercial hybrid inverters reveals performance gaps:

- Commercial MPPT efficiency: 97-99% vs. 87% (LM317)
- Commercial inverter THD: 3% vs. 43% (square-wave)
- Commercial battery management: Active BMS vs. passive voltage monitoring
- System efficiency: 85-92% (commercial) vs. 62% (prototype)

However, prototype achieves 70% cost reduction and serves educational objectives effectively.

## IX. RECOMMENDATIONS

### A. Immediate Improvements

**Switched-Mode Charger:** Replace LM317 with buck converter achieving 92-95% efficiency and eliminating heat dissipation issues. Synchronous rectification further reduces conduction losses.

**SPWM Inverter:** Implement H-bridge topology with microcontroller-generated SPWM reducing THD to 3%. Digital control enables advanced features including soft-start, overload protection, and islanding detection.

**Microcontroller Integration:** ESP32 or STM32 platform enables:

- Adaptive threshold adjustment based on battery characteristics
- Data logging and wireless telemetry
- Time-of-day load scheduling
- Predictive maintenance alerts
- Remote monitoring and control

### B. Advanced Enhancements

**Lithium-Ion Integration:** Migrate to lithium-ion batteries with proper BMS providing:

- 2000-5000 cycle life (4-10× lead-acid)
- Cell balancing preventing capacity degradation
- Thermal management and safety protection
- State-of-health monitoring

**MPPT Optimization:** Implement perturb-and-observe or incremental conductance algorithms maximizing PV energy harvest across varying irradiance conditions [1].

**Machine Learning Integration:** Deploy predictive models for:

- Generation forecasting using weather data
- Anomaly detection identifying degradation or faults
- Optimal scheduling minimizing grid dependence
- Predictive maintenance reducing unplanned downtime

**Grid-Interactive Operation:** Add synchronization capability for:

- Net metering with utility grid
- Peak shaving during high-tariff periods
- Demand response participation
- Emergency backup seamless transfer

## X. CONCLUSION

This work presented comprehensive design, implementation, and evaluation of a data-enhanced solar hybrid charging system demonstrating practical viability for distributed energy applications. The prototype successfully integrated dual charging sources, automatic load prioritization, and analytics-driven performance monitoring while maintaining affordability through judicious component selection.

Hardware validation confirmed 62% overall system efficiency with reliable load switching across three priority levels. Power BI analytics revealed seasonal performance patterns and substantial economic benefits, with monthly savings ranging from 43.93k to 62.33k rupees. The system effectively demonstrated core hybrid energy management principles suitable for rural electrification and emergency backup scenarios.

Identified limitations including linear regulator inefficiency, square-wave inverter output, and passive battery management provide clear pathways for enhancement. Recommended improvements through switched-mode power conversion, SPWM

topology, and microcontroller integration offer substantial performance gains while maintaining cost-effectiveness.

Future work will focus on advanced battery management integration, machine learning-based optimization, and field deployment validation in actual rural settings. The combination of renewable generation, intelligent storage management, and data analytics positions hybrid systems as critical enablers of sustainable, resilient energy infrastructure for underserved communities.

## REFERENCES

- [1] A. K. Abdelsalam, A. M. Massoud, S. Ahmed and P. N. Enjeti, "High-Performance Adaptive Perturb and Observe MPPT Technique for Photovoltaic-Based Microgrids," *IEEE Transactions on Power Electronics*, vol. 26, no. 4, pp. 1010–1021, Apr. 2011.
- [2] S. B. Kjaer, J. K. Pedersen and F. Blaabjerg, "A Review of Single-Phase Grid-Connected Inverters for Photovoltaic Modules," *IEEE Transactions on Industry Applications*, vol. 41, no. 5, pp. 1292–1306, Sept.–Oct. 2005.
- [3] B. K. Bose, "Global Energy Scenario and Impact of Power Electronics in 21st Century," *IEEE Transactions on Industrial Electronics*, vol. 60, no. 7, pp. 2638–2651, Jul. 2013.
- [4] J. M. Carrasco et al., "Power-Electronic Systems for the Grid Integration of Renewable Energy Sources: A Survey," *IEEE Transactions on Industrial Electronics*, vol. 53, no. 4, pp. 1002–1016, Jun. 2006.
- [5] M. J. Khan and M. T. Iqbal, "Pre-feasibility study of stand-alone hybrid energy systems for applications in Newfoundland," *Renewable Energy*, vol. 30, no. 6, pp. 835–854, 2005.
- [6] D. Linden and T. B. Reddy, *Handbook of Batteries*, 4th ed. New York: McGraw-Hill, 2010.
- [7] M. H. Rashid, *Power Electronics: Devices, Circuits and Applications*, 4th ed. London: Pearson, 2017.
- [8] G. M. Masters, *Renewable and Efficient Electric Power Systems*, 2nd ed. Hoboken, NJ: Wiley, 2013.
- [9] M. R. Patel, "Wind and Solar Power Systems: Design, Analysis, and Operation," 3rd ed. Boca Raton, FL: CRC Press, 2020.